Multi-point Forming Springback Compensation Control of Two-dimensional Hull Plate

Shaojuan Su [1, 2]*, Yuchao Jiang [1],Yeping Xiong[2]
([1]Naval Architecture and Ocean Engineering College,
Dalian Maritime University, 116026, Dalian Liaoning, China;
[2]Faculty of Engineering and Physical Sciences, University of Southampton, Boldrewood Innovation Campus, SO16 7QF Southampton, UK)

Abstract: Springback is always a technical problem in sheet metal forming. In this paper, the rapid springback compensation control of two-dimensional hull plate is realized by theoretical calculation and numerical simulation. For the cylindrical shell, according to the bending forming theory of medium and thick plates, the total elastic-plastic bending moment is established, and the curvature change before and after springback is deduced. The curvature correction coefficient is determined by the precise numerical simulation technology. At the same time, the validity of the method is verified by cold bending experiment. For the shell with variable curvature, it is divided into several cylindrical surfaces according to the curvature gradient of its geometric section line. The compensation curvature array is obtained by the correction compensation algorithm of springback curvature of cylindrical plate, and the algorithm is verified by numerical simulation. The results show that the method is very close to the expected results. Thus, the efficiency and precision of forming will be improved, and the foundation of digitization of sheet metal forming is established.
Key words: springback compensation; surface reconstruction; numerical simulation; two-dimensional shell; forming theory

Introduction

The formation of hull shells, especially of large curved shells, has always been a most difficult problem in the field of plastic hull processing. The simple and effective shaping of ship plates with different thicknesses and curvatures to meet design requirements has always been the development direction of hull plate-forming technology. For a long time, two-dimensional parts, such as cylindrical and conical parts, have been formed by rolling or bending shown in Figure 1.[1-2] When the bending resistance of the roller is relatively large, the roller will be distorted and deformed so that the processed workpiece is in the shape of a barrel. Therefore, when roller process a relatively thick material with a relatively high material strength, it is necessary to increase the support or make the shape of the roller barrel offset the effect of its deformation.[3] At the same time, the traditional symmetrical three-roller coiling machine has a straight edge problem at both ends of the sheet, so the sheet material is pre-bent.[4] Three-dimensional curved parts are mostly formed by water-fired curved plates, but there are many problems with this approach, such as high labor intensity, high requirements for workers, and low production efficiency. With the development of the computer numerical control (CNC) cold bending machine, multi-point CNC cold press forming has gradually become the main process in sheet metal forming.[5] The asymmetric stamping square head adjustable die shown in Figure 2, developed by Wuhan University of Technology in China in 2012, can solve the indentation and wrinkling problems that easily occur in the cold forming process; at the same time, compared to the overall die, the height of each basic body punch can be arbitrarily adjusted, and the envelope surface of different shapes can be quickly formed, and the springback of the sheet forming can be compensated by correcting the shape of the envelope surface, that is, the die-repairing process of the whole die is omitted. Multi-point forming has the advantage of reducing costs, increasing production efficiency, and automating the forming process.[6] However, calculating springback has always been a technical problem in sheet metal forming.

Hill[7] firstly established the exact mathematical theory of plate bending by proposing the basic theory of elastoplastic bending under plane-strain conditions and deducing the complete solution without considering the hardening of materials under pure bending conditions. Wenner[8] studied the work of hardening and the springback of sheet metal forming under plane strain. Chu[9] pointed out that the sidewall part experienced a complex bending-draw process during the forming process when

he analyz the springback problem of U-shaped parts. Based on the uniform deformation and plane-strain conditions, the isotropic follow-up hardening model was adopted. The effects of in-plane restraint, materials, and process parameters on springback were analyzed. Wang[10] studied the bending springback problem of V-shaped parts and established a bending moment with material strength coefficient, a hardening index, a thickness anisotropy coefficient, plate thickness, plate width, and the convex die fillet as independent variables. The model is used to predict springback, formability, stress and strain distribution, and maximum die load during sheet metal forming. Wagoner[11] established some mechanical models for describing and calculating springback predictions. Braga[12] established a theoretical model of springback prediction based on an elastic pad, and its feasibility was verified through experimentations. Oliveira et al.[13] used the questions in NUMISHEET2005 as an example to study the effects of different work hardening models on the accuracy of springback prediction, indicated that the selection of material strengthening models can affect springback results. Marko[14] proposed a thin-plate pure bending mechanics model that considered the thickness anisotropy coefficient r and the hardening exponent n to evaluate springback, bending, and the maximum bending moment. Chen[15] carried out theoretical calculation to calculate single curvature springback and the surface reconstruction is carried out by NURBS.

From the above research, the traditional analytical method has made numerous assumptions and simplifications in solving the springback problem, but it rarely considered the influence of process parameters on springback during the actual forming process, which brings a large error to the calculation results. In this paper, based on the theory of medium-thickness plate bending, the theory of cylindrical and conical hull shell forming springback is discussed in detail. Based on this, an asymmetric stamping square head adjustable die forming simulation model is established. The accurate numerical simulation method is used to correct the springback curvature to effectively control springback and improve forming precision.

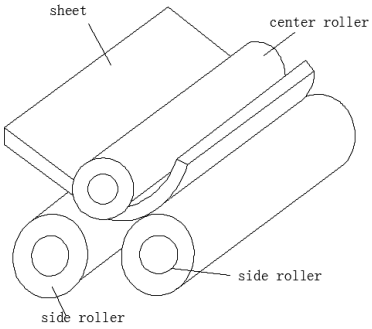

Figure 1. Roll forming

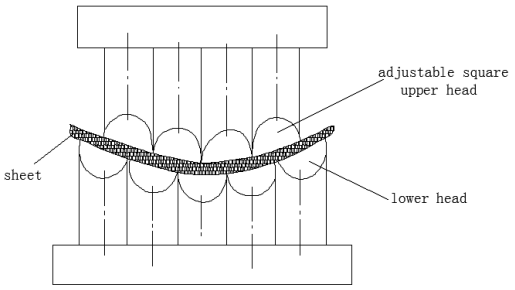

Figure 2. Asymmetric stamping square head adjustable die

1 Theoretical Calculation Model

The calculations of springback are based on the theorem that the distortion caused by the unloading of a force or moment is equal to the deformation caused by the loading of a force or moment of the same magnitude but opposite direction. Therefore, the accuracy of the springback calculation depends on the accuracy of the force's or moment's calculations, as well as the accuracy of the moment of inertia calculations.[16]

1.1 Basic assumption

According to the bending forming theory of medium and thick plates, the inner material elements stress and strain are determined by the width(W)-thickness(t) ratio W/t and the relative bending curvature $\bar{k}$.[17]

When $\bar{k} < 0.1$ and $W/t > 8$, horizontal warpage of the sheet is ignored, the plate is in elastoplastic deformation. The material in the inner elastic zone is subjected to unidirectional stress, the material in the outer plastic zone is in plane strain and the neutral layer is not moved. In line with the bending engineering theory, the thickness reduction can be neglected.

Meet the following basic assumptions:

1) Plate bending process is pure bending[16];

2) It only undergoes elastic deformation and elastoplastic deformation, it does not undergo plastic

deformation, and it satisfies the plane strain condition, so that, the strain in the width direction $\varepsilon_b = 0$ and the variation of the thickness can be neglected[17];

3) There is no extrusion between the longitudinal fibers of the plate during the bending process, and there is no transverse stress between the fiber layers, and each fiber in the slat is in a uniaxially stretched or uniaxially compressed stress state;

4) The intermediate layer and the neutral layer are coincident. According to the mathematical theory of plastic bending, under the condition of pure bending, when the bending radius of the center layer of the plate is greater than 10 times thickness, the difference between the intermediate layer and neutral layer can be neglected, and the forming process of the bilge of the hull meets these conditions.

1.2 Mathematical model

Using the power-function stress-strain mathematical model to approximate the true stress-strain relationship of the material, [18] the stress-strain relationship of the material is shown in formula (1) and Figure 3.

$$\sigma = \begin{cases} E \cdot \varepsilon & 0 < |\varepsilon| \le \varepsilon_e \\ \sigma_0 + K\varepsilon^n & |\varepsilon| > \varepsilon_e \end{cases} \tag{1}$$

where σ is the true stress of the steel, σ_0 is the yield strength of steel, K is the hardening coefficient and n is the hardening index, E is elastic modulus, ε_e is the strain value at which the material yields initially.

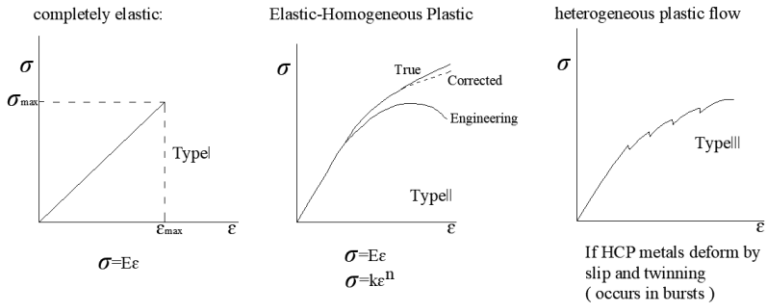

Figure 3. Stress strain curve

As shown in Figure 4, the material in the inner and outer shadow portions of the ship plate is plastically deformed, and the material in the middle portion is elastically deformed.[16]

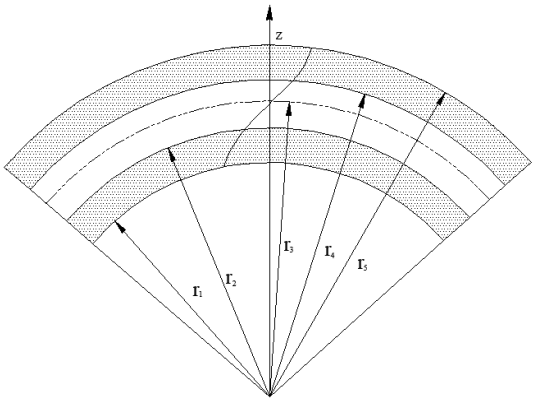

Figure 4. three zones of plate during bending

$$\begin{cases} r_4 = (1+\varepsilon_e)r_3 \\ r_2 = (1-\varepsilon_e)r_3 \end{cases} \tag{2}$$

1) Moment of elastically deformation zone

According to the theory of metal bending forming, [19] the internal strain of the plate is shown in formula (3) and the bending moment is shown in formula (4).

$$\varepsilon = \frac{r - r_3}{r_3} = \frac{r}{r_3} - 1 \tag{3}$$

$$M = b\int_{r_2}^{r_4} \sigma (r - r_3) dr \tag{4}$$

where M is the bending moment, $r_3 = \frac{1}{k}$, b is the width of the plate, r is the radius of any lamellar parallel to the intermediate layer.

Submit (1) (2) (3) into (4), and obtain the bending moment of the elastic deformation region.

$$\begin{aligned} M_{2,4} &= b\int_{r_2}^{r_4} \sigma (r - r_3) dr = b\int_{r_2}^{r_4} E\varepsilon (r - r_3) dr \\ &= b\int_{r_2}^{r_4} E\left(\frac{r}{r_m} - 1\right)(r - r_3) dr = \frac{2}{3} E\varepsilon_e^2 r_3^2 b \end{aligned} \tag{5}$$

2) Moment of elastoplastic deformation zone

Moment of plastic deformation zone on the outer side of ship plate

$$M_{4,5} = b\int_{r_4}^{r_5} \sigma_\theta (r - r_3) dr \tag{6}$$

According to the plate strain assumption and the material incompressibility condition, $\bar{\varepsilon} = 2\varepsilon_\theta / \sqrt{3}$. And according to the plane strain and the Mises yield strain criterion, $\sigma_\theta - \sigma_r = 2\bar{\sigma} / \sqrt{3}$, where ε_θ is the longitudinal strain, σ_θ is the longitudinal stress, σ_r is the radial stress and $\bar{\sigma}$ is the equivalent stress.[20] When the plate is in elastoplastic bending deformation, the degree of bending deformation is small, the longitudinal stress of the material unit is much larger than the radial stress, and the longitudinal stress of the material unit is:

$$\sigma_\theta \approx 2\bar{\sigma} / \sqrt{3} \tag{7}$$

Submit (1) into (7) and obtain the plastic deformation zone to obtain the stress:

$$\sigma_\theta \approx 2\bar{\sigma} / \sqrt{3} = 2 / \sqrt{3} (\sigma_0 + k\varepsilon^n) \tag{8}$$

Submit (1) (2) (8) into (6)

$$\begin{aligned} M_{4,5} &= b\int_{r_4}^{r_5} \sigma_\theta (r - r_3) dr = b\int_{r_4}^{r_5} 2/\sqrt{3} (\sigma_0 + k\varepsilon^n)(r - r_3) dr \\ &= \frac{b\sigma_0}{\sqrt{3}} \left[\left(\frac{t}{2}\right)^2 - (\varepsilon_e r_3)^2\right] + \frac{2bk}{\sqrt{3}(n+2) r_3^2} \left[\left(\frac{t}{2}\right)^{n+2} - (\varepsilon_e r_3)^{n+2}\right] \end{aligned} \tag{9}$$

3) Before springback curvature

The total bending moment of the elastoplastic bending is formula (10).

$$M = M_{2,4} + 2M_4 \tag{10}$$

The change in curvature due to springback is [19]:

$$\Delta k = \frac{M}{E \times I} \tag{11}$$

$$k_1 = k_2 + \Delta k \tag{12}$$

where k_1 is the curvature before springback, k_2 is the curvature after springback and Δk is the curvature change.

It can be known from the formula (12) that for a plate having a single curvature shape, if the

material parameters, the thickness, and the target curvature are known, the springback curvature value after unloaded can be predicted. Similarly, the curvature of the target surface is taken as the curvature after springback. The curvature before springback of the upper and lower basic groups can be obtained which will improve the springbact effect by changing the target curvature.

4) Curvature correction coefficient

The theoretical model is based on some assumptions, which the actual springback process is affected by material parameters and process parameters (such as punching pressure, friction state, stamping speed, stamping displacement, etc.). Therefore, there will be a deviation between the actual stamping and the predicted curvature. Here, accurate numerical simulation technology is used instead of experiment.[21] Calculate the curvature correction coefficient η .

$$\eta = \frac{k^m}{k^t} \Rightarrow k^m = \eta \cdot k^t = \eta \cdot (k + \Delta k) \tag{13}$$

where k^m is springback curvature by numerical simulation; k^t is the springback curvature by theoretical prediction; k is the target curvature; Δk is the curvature deviation.

2. Surface reconstruction technology based on NURBS

2.1 Discrete curvature

According to the curves differential geometry theory, [22] discrete the geometric section curve of any shape plate into a segment arc and use the curvature ratio before and after springback of each arc to characterize the springback. Each discrete unit uses the bending theory to predict the curvature after springback and is corrected by the numerical simulation result. The discrete curvature of the compensation die surface required for the next pressing is obtained. Reconstruct the compensation surface and get the ideal part by trimming die and re-punching.

The key of this method is to transform the springback problem of complex irregular section stamping into the springback problem of regular equal curvature by discrete method, obtain the compensation curvature array by curvature correction compensation algorithm. Finally, the compensation surface is reconstructed from the differential geometry algorithm of the curved curve based on the curvature data.

The bilge shells at the non-parallel middle body usually have conical surface. It can be discretized into n cylindrical surface according to the gradient of the curvature of its geometric section line. When n is relatively large, it can be considered that each small segmented curve's is an equal curvature arc, and the plate is discrete into n cylindrical surfaces. Set the curvature of the center point of each arc to the average curvature of the arc. Finally, the geometric model of the compensation surface of the whole curvature part is obtained by using the discrete arc length curvature data of each small segments, and the initial die surface is corrected according to the geometric model.

2.2 Discrete data

Assume that the curvature of two adjacent discrete points has been calculated, and the arc length between the two points is $\Delta s (\Delta s = s_{i+1} - s_i)$. Suppose the curvature between two adjacent discrete points is linear with the arc length shown in equation (14).

$$k = m \times s + n \tag{14}$$

where m and n are two coefficients. In order to determine the value of m and n, the curvature of two adjacent discrete points k_i, k_{i+1} can be substituted into equation (15).

$$\begin{cases} k_{i+1} = m \times s_{i+1} + n \\ k_i = m \times s_i + n \end{cases} \tag{15}$$

The formula (16) can be solved by equation (15)

$$\begin{cases} m = (k_{i+1} - k_i) / (s_{i+1} - s_i) \\ n = (k_i \times s_{i+1} - k_{i+1} \times s_i) / (s_{i+1} - s_i) \end{cases} \tag{16}$$

According to the differential geometry of the curve, equation（17）is known.

$$\varphi = \int k(s)ds = \int (m \times s + n)ds = \frac{1}{2}m \times s^2 + n \times s + c \tag{17}$$

For the curve between two adjacent discrete points, the segmented curve can be further divided into a plurality of small arc segments. For the $i-th$ segments, the expression of the curvature is obtained from equation (15), and then according to the integral equation (17) to obtain the expression of the equation (18).

$$\begin{cases} k_i = m \times s_i + n \\ \varphi(s_i) = \frac{1}{2} \times m \times s_i^2 + n \times s_i + c \end{cases} \tag{18}$$

Then in the $i-th$ segment, the equation (19) is established.

$$\begin{cases} \theta_i = \Delta s / \rho_i = \Delta s \times k_i \\ ds_i = 2 \times \sin(\theta_i / 2) / k_i \quad (k_i \neq 0) \\ ds_i = \Delta s \qquad\qquad\qquad (k_i = 0) \\ \Delta x_i = ds_i \times \cos(\varphi_i + \theta_i / 2) \\ \Delta y_i = ds_i \times \sin(\varphi_i + \theta_i / 2) \end{cases} \tag{19}$$

See Figure 5, where ρ_i, ρ_{i+1} is the radius of the curvature at two adjacent points P_i, P_{i+1} on the curve, the corresponding curvature is k_i and k_{i+1}. Δs and ds_i the arc length and chord length. θ_i is the corresponding central angle and $\Delta x_i, \Delta y_i$ is the coordinate increment of P_{i+1} relative P_i.

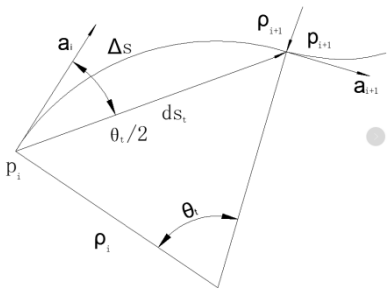

Figure 5. Recursive curve position by curvature integral

Then get the coordinate recursion equation (20) from P_i to P_{i+1}.

$$\begin{cases} x_{i+1} = x_i + \Delta x_i \\ y_{i+1} = y_i + \Delta y \end{cases} \tag{20}$$

According to equation (20), the position of the curve can be obtained point by point.[23]

2.3 Discrete Point Surface Reconstruction Based on NURBS

The NURBS surface equation obtained by the parameters in μ, ν directions are shown in equation (21).

$$S(u,v) = \frac{\sum_{i=0}^{n}\sum_{j=0}^{m} \varpi_{i,j} d_{i,j} N_{i,k}(u) N_{j,l}(v)}{\sum_{i=0}^{n}\sum_{j=0}^{m} \varpi_{i,j} N_{i,k}(u) N_{j,l}(v)} \tag{21}$$

where $d_{i,j}$ is the control grid point of the matrix composed of discrete points S^{point}; $\varpi_{i,j}$ is a set of weight factors greater than 0 associated with $d_{i,j}$; $N_{i,k}(u)$ is the k-direction spline function in the μ direction; $N_{j,l}(v)$ is the L-order spline function in the ν direction, where the basic functions of the surface and the curve are the same.[24]

In this paper, the NURBS method is used and the surface is controlled by the control points obtained in Section 2.2, so that the shape of the surface can be flexibly changed by editing the

control points, and the discrete nodes are fitted into curves by NURBS method. Which can improve the smoothness of the curve and get a smoother surface. CATIA software[25] is selected to surface reconstruction, which facilitates the processing of the generated surface in the subsequent steps, ensuring the consistency of the surface in the design and manufacturing process.

Springback compensation control flow chart based on NURBS is shown in Figure 6.

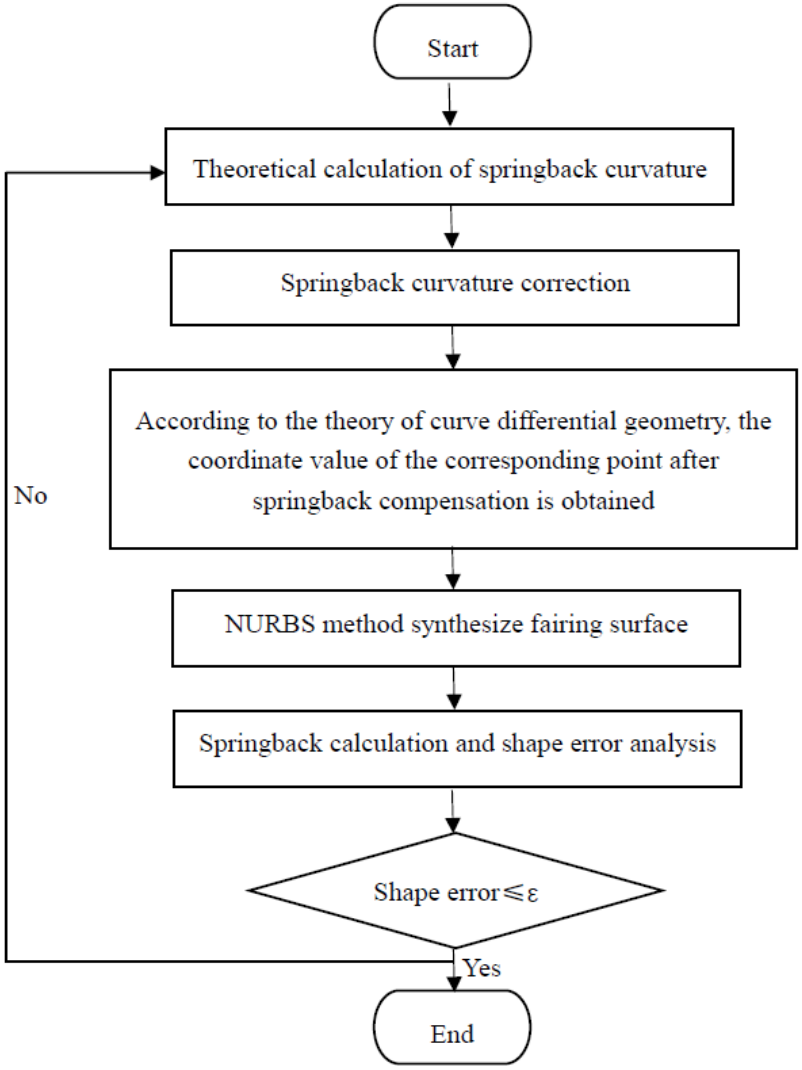

Figure 6. Springback compensation control flow chart

3 Example of equal curvature springback compensation control

3.1 Numerical simulation

In order to obtain the springback curvature correction coefficient, the numerical simulation of the cylindrical sheet with a curvature radius of 2000 mm is carried out. The key techniques of numerical simulation are as follows.

3.1.1 Establishment of 3D model

Solidworks is used to establish a 3D model of finite element multi-point forming. There is a rotating spherical crown under the square head die, which allows the head to swing freely. In the contact stage the remaining parts are not in contact with any part, except the upper surface of the square head is in contact with the sheet. In order to save the modeling workload and calculation time, the spherical crown behind the square head is simplified shown in Figure 7. The upper dies and the lower dies adopt a misalignment distribution. The model is established shown in Figure 8.

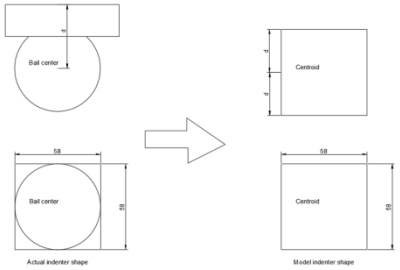

Figure 7. Simplify the head die process

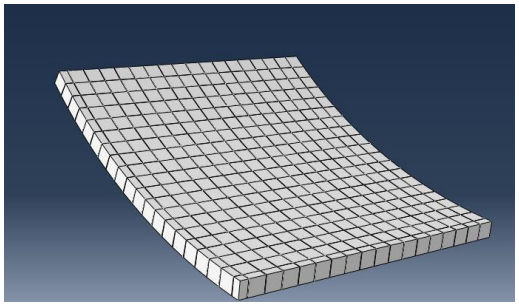

Figure 8. The die models

3.1.2 Material properties

In the multi-point forming analysis, during the forming process the deformation of the die is small, so it is treated as a rigid body. The elements of the rigid body material are not involved in the calculation of stress and strain, and the elastic modulus and Poisson's ratio are mainly used to calculate the contact force on the surface when the sheet and the die come into contact. The plate material parameter settings are shown in Table 1.

Table 1. Properties of material

R(mm)	B(mm)	t(mm)	L(mm)	σ_s / *MPa*	E/GPa	λ	K	n
2000	2000	16	2000	345	206	0.3	630.3	0.236

In Table 1. R is cylindrical plate radius of curvature; B is shell width; L is shell length; t is shell thickness; σ_s is yield strength; E is elastic modulus; λ is poisson's ratio; K is hardening coefficient and n is hardening index.

3.1.3 Contact conditions

The contact mode between the die and the sheet is universal contact. The friction model directly affects the calculation accuracy. The modified Coulomb friction model is used in the paper.[25] this is a friction model that has been proved to be more realistic in practice. The friction coefficient is set to 0.1 in the paper.

In the springbcak phase, in order to visually observe the springback displacement of the plate, the center point of the plate is rigidly fixed to avoid unnecessary displacement.

3.1.4 Unit and meshing

The plate is made of a structural hexahedron mesh, and the number of meshes is divided. The number of meshes with 1000mm lengths on both sides is 100 and the thickness direction is 4 shown in Figure 9.Since the upper and lower dies are rigid bodies, in order to reduce calculation, the mesh size is 11.6 mm and the maximum deviation factor is 0.1.The upper die mesh is shown in Figure 10.The forming stage unit type is selected as explicit, linear geometric order, C3D8R eight-node linear hexahedral element, reduced integral and hourglass control. The springback phase unit is selected as implicit, linear geometric order, C3D8R eight-node linear hexahedral element, reduced integral and hourglass control.

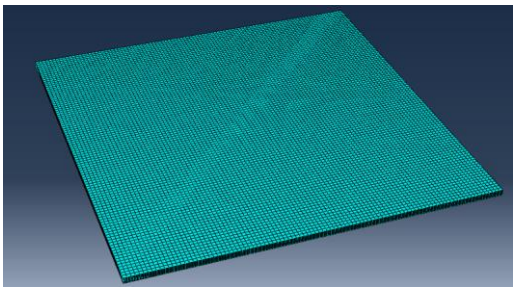

Figure 9. Meshing of plate

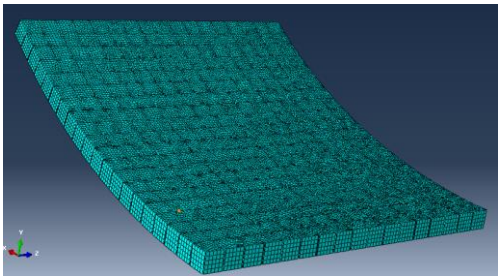

Figure 10. Meshing of upper die

3.1.5 Calculation results Analysis

The displacement distribution cloud after springback is shown in Figure 11. The maximum springback displacement is 45.47mm. The radius of the curvature after springback is 2412.4 mm by geometric calculation.

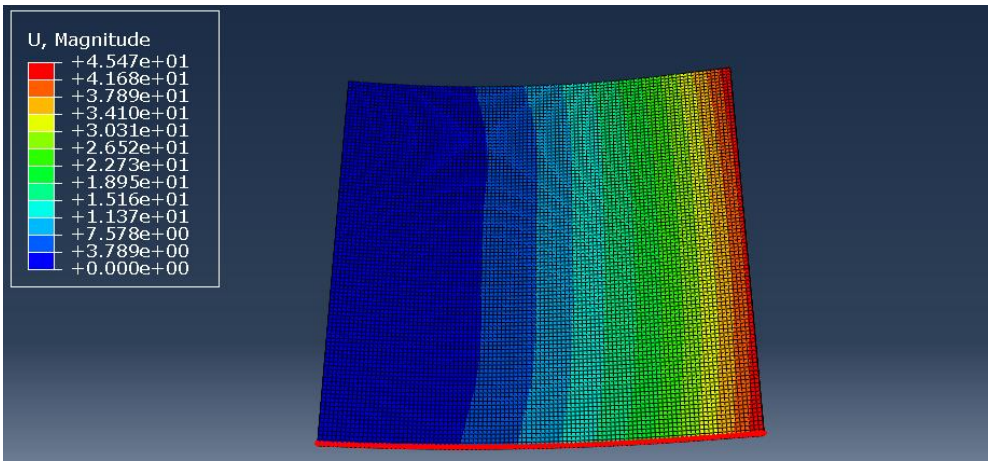

Figure 11. Displacement distribution cloud after springback

3.2 The springback curvature correction coefficient

It can be seen from the Figure 11 that the springback gradually increases from the center to the edge of the shell and the maximum springback is 45.47 mm. The spline curve is obtained with a radius of curvature of about 2412mm after springback. Using the above theoretical study, the target radius of curvature is 2412mm and the radius of the curvature before springback should be 1923mm. Curvature correction coefficient is 1.040. In order to improve the calculation accuracy, five sets of data are selected to average shown as Table 2, finally select the springback curvature correction coefficient is 0.982

Table 2. Springback curvature correction coefficient

radius of curvature before springback`	2500	2200	2000	1800	1500
correction coefficient	1.026	1.023	0.971	0.941	0.949

3.3 Numerical simulation verification

According to formulas (5), (9), (10), (11), (12) and (13), the radius of the curvature of the Q345 plate with a target curvature of 2000 mm is calculated to be 1677 mm. In order to verify the accuracy of the theoretical calculation method, numerical simulation method is use to verify the Validation. The calculation results are shown in Figure 12. It can be seen from the figure that the curvature radius before springback is calculated by the method in this paper, and the curvature after springback is very close to the target curvature.

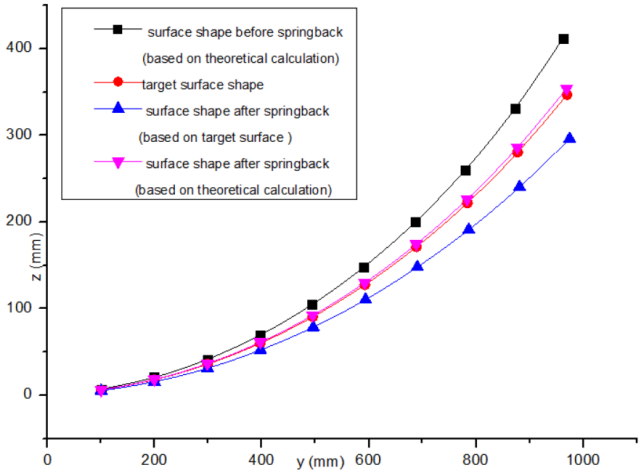

Figure 12. Forming result shape comparison

3.4 Experimental verification

The springback experiment of Q345 plate with a curvature radius of 1677mm was carried out. Import the prepared experimental data into the instrument, and the instrument will automatically adjust the position of the lower dies according to the data. After the completion of the profile adjustment, the lower dies will form a certain curved surface, as shown in Figure 13.

Figure 13. The lower dies curved surface

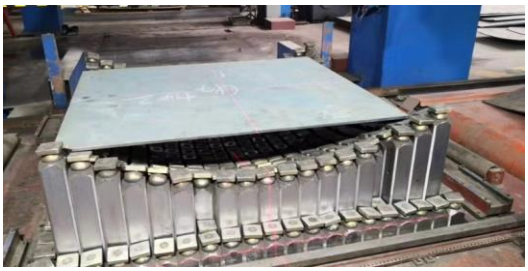

Figure 14. The plate on the lower dies

In the process of shape adjustment, the indenter moves vertically, the indenter plane is horizontal, and the surface formed is not completely smooth. In the process of pressing, the indenter will rotate under the force of the upper indenter and finally fit into a better surface. Then fix the plate on the formed die, as shown in Figure 14, and operate the upper indenter to lower and compact, as shown in Figure 15. After pressing, keep the pressure for a certain period of time to prevent the plate from springback immediately. The effect after pressing is shown in Figure 16. It can be seen that the non-symmetric pressure head can still be successfully fitted into a suitable surface. In addition, compared with other types, there is no need to add special blank holder around the plate.

Figure 15. Plate is compacted by dies

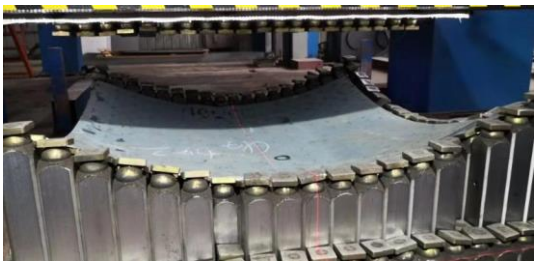

Figure 16. The effect after pressing

The measurement is carried out after pressing. Figure 17 shows the comparison between the measurement results of the laser measuring instrument and the target surface. Red is the measurement value and black is the theoretical value. The other is to measure on the surface with the already made template. Figure 18 is to measure with the template.

After forming, the curvature radius after springback measurement is 2025mm. The radius of curvature is 2000 mm after theoretical calculation. So, 98.77% accuracy is satisfied the technological requirements.

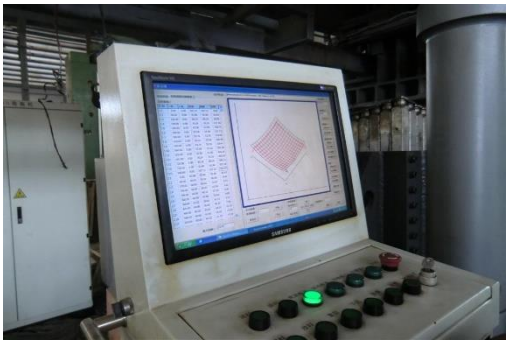

Figure 17. Measurement results of the laser

Figure 18. Measure with the template

4 Example of variable curvature springback compensation control

The bilge of a ship in a non-parallel middle body is a conical surface. Its properties of material is same as Table 1. The partially discrete curvature along the length direction is shown in Table 5. The target shape is shown in Figure 19.

Table 5. Partially discrete curvature along the length direction

x	0	200	400	600	800	1000	1200	1400	1600	1800	2000
radius of curvature	2000	1950	1900	1850	1800	1750	1700	1650	1600	1550	1500

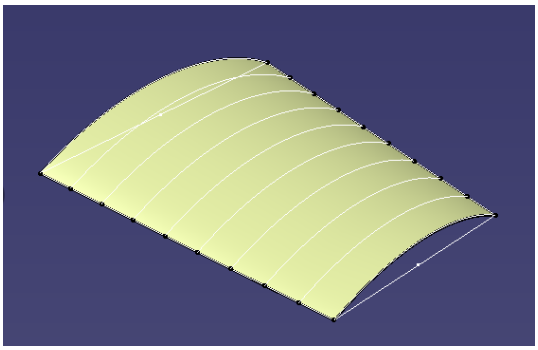

Figure 19. Target surface shape

The linear interpolation method is used to discretize the curvature. Based on the two-dimensional springback calculation theory, the radius of the curvature before springback of each discrete section is obtained, and the above-mentioned curvature-based surface reconstruction method is used to obtain the discrete points. Some data are shown in Table 6. CATIA method is used for surface reconstruction [26] shown in Figure 20. The surface shape before and after springback are shown in Figure 21.

Table 6. Discrete data points before springback

						X=0					
y	0	99.87	199.46	298.67	397.40	495.51	592.88	689.36	784.77	878.92	971.57
z	0	5.90	17.73	35.55	59.47	89.63	126.23	169.55	219.92	277.76	342.45
						X=200					
y	0	97.87	197.47	294.68	391.42	487.57	582.99	677.55	771.08	863.38	954.23
z	0	5.78	17.73	35.30	58.85	88.52	124.52	167.10	216.61	273.47	337.69
						X=400					
y	0	95.87	195.47	290.69	385.44	479.62	573.09	665.72	757.36	847.81	936.85
z	0	5.66	17.74	35.07	58.26	87.46	122.85	164.71	213.38	269.27	332.90
						X=600					
y	0	93.88	193.47	286.70	379.46	471.66	563.18	653.88	743.62	832.20	919.42
z	0	5.55	17.76	34.86	57.70	86.43	121.24	162.39	210.23	265.18	328.11
						X=800					
y	0	91.88	191.48	282.70	373.47	463.70	553.26	642.02	729.85	816.57	901.95
z	0	5.43	17.79	34.67	57.17	85.43	119.67	160.14	207.17	261.19	323.30
						X=1000					
y	0	89.88	189.48	278.70	367.49	455.73	543.32	630.15	716.06	800.89	884.43
z	0	5.32	17.84	34.49	56.66	84.48	118.16	157.95	204.19	257.31	318.48
						X=1200					
y	0	87.89	187.49	274.71	361.49	447.75	533.38	618.26	702.25	785.19	866.87
z	0	5.21	17.90	34.34	56.18	83.57	116.69	155.82	201.29	253.53	313.65
						X=1400					
y	0	85.89	185.49	270.71	355.50	439.77	523.43	606.35	688.42	769.45	849.27
z	0	5.10	17.97	34.21	55.74	82.70	115.29	153.77	198.49	249.87	308.81
						X=1600					
y	0	83.89	183.50	266.71	349.50	431.78	513.46	594.43	674.56	753.68	831.61
z	0	4.99	18.07	34.11	55.33	81.87	113.94	151.79	195.77	246.31	303.95

						X=1800					
y	0	81.89	181.50	262.70	343.49	423.79	503.49	582.49	660.67	737.88	813.92
z	0	4.89	18.18	34.02	54.95	81.09	112.65	149.89	193.15	242.87	299.09
						X=2000					
y	0	79.89	179.50	258.70	337.49	415.78	493.50	570.53	646.76	722.04	796.17
z	0	4.78	18.31	33.97	54.60	80.35	111.41	148.06	190.62	239.54	294.20

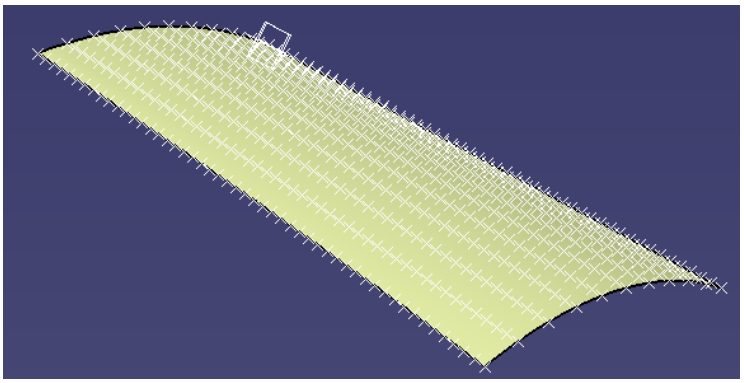

Figure 20. Curved surface shape before springbcak

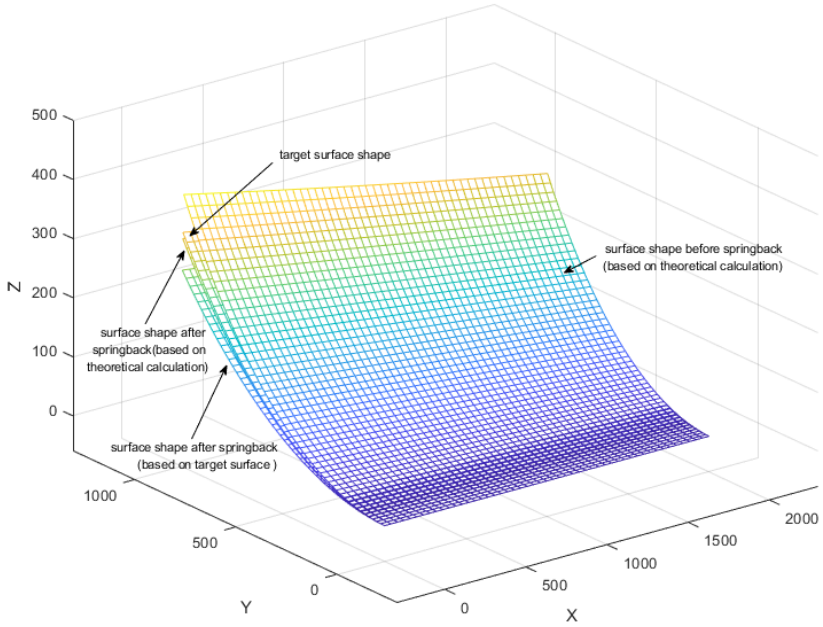

Figure 21. Surface shape before and after springback

5 Conclution

Although the theory of two-dimensional sheet metal forming is a traditional topic, with the continuous development of mechanization, intelligence and simulation technology, the forming equipment is constantly updated. The theoretical calculation model of sheet metal forming is corrected based on the advanced equipment of asymmetric pressure square head CNC cold bending machine. The following conclusions can be obtained by calculations.

We can find the theoretical springback formula has a certain range of application, from equation (9). When the radius of the curvature is greater than 4770mm, the plastic deformation is small and the moment of plastic deformation zone on the outer side of ship plate is negative value. The formula will no longer apply.

Forming theory is unlikely to produce very accurate springback results, but it is very close to the desired result, so that the times of stamping can be reduced as much as possible and improve the

processing efficiency.

In addition, the results of theoretical analysis and simulation need to be verified by a large number of experiments. The theoretical model and the finite element model should be corrected by the results of the experiments and finally a more accurate model will be obtained. Due to time and cost, only some experimental data have been added in the paper. In the next work, we will use more experimental data, accurate numerical simulation algorithm, and try to apply the theory and method of two-dimensional sheet metal forming to three-dimensional sheet metal forming.

Declaration of conflicting interests

The author (s) declared no potential conflicts of interest with respect to the research,authorship,and/or publication of this article.

Funding

The author(s) disclosed receipt of the following financial support for the research, authorship, and/or publication of this article: The work presented is supported by Natural Science Foundation of China (51609031) and China Scholarship Council (No.201806575010).

ORCID ID

Shaojuan Su https://orcid.org/0000-0001-9654-0359

References

[1] Meng S F. Theoretic analyses and numerical simulation of three-roll pyramid type plate bending machine bending process. *MA Thesis, Jiangsu University*, China, 2006.

[2]Wang, Y; Zhao, L L; Cui, X M. Research on numerical simulation and process parameters of three-roll bending based on thickness characteristics of extra-thick plate. *Advances in mechanical engineering*.2019; 11(4): 1–10.

[3] Jin G M. Causes and corresponding measures of barrel deformation during coiling process. *Metal forming technology*. 1999; 17(2):28-30.

[4] Chen Y X. *Principle and method of bending and springback control of sheets and profiles.* National Defense Industry Press, 1980

[5] Su S J,Hu Y,Wang C F. Research progress of three-dimensional plate forming method for ship hull. *Shipbuilding of China*.2012; 53(2):211-216.

[6] Wang C F, Hu Y, Li J X, et al. A novel forming method for 3D ship hull forming. *Journal of Wuhan University of Technology*.2010; 34(3):431-434.

[7] R.Hill. The Mathematical Theory of Plasticity. Oxford, London, 1950.

[8] Wenner M L. On Work Harding and Springback in Plane Strain Draw Forming. *Applied Metalworking*.1993; 12(4) 277-287.

[9] Chu C C. The effect of restraining force on springback. *International Journal of Solids and Structures*.1991; 27(8): 1035-1046

[10] Wang C., Kinzel G., Altan T. Process simulation and springback control in plane strain sheet bending, SAE Technical paper .1993;930280

[11] Wagoner R H, LI M, Gan W. Sheet springback: prediction and design. *HSIMP 2007: high speed industrial manufacturing processes, Cetim*, 2007:1-7.

[12] Braga M T, Moreira L A. Springback analysis of thin bent sheets on elastomeric die. *Int J Mater Form*.2010; 3:1075-1078.

[13] Oliveira M C, Alves J L, et al. Study on the influence of work-hardening modeling in springback prediction. *International journal of plasticity*. 2007;23(3):516-543.

[14] Marko V, Miroslav Halilovič, et al. A new anisotropic elasto-plastic model with degradation of elastic modulus for accurate springback simulations. *Int J Mater Form*.2011; 4:217-225.

[15] Chen Y D.Numerical simulation study on the springback control of multi-point forming for curved hull plate.Jinlin university, China. 2015:27-39

[16] Zhang Z T and Lee D. Development of a new model for plane strain bending and springback analysis. *Journal of material engineering and performance*.1995; 4:291-300.

[17] Ma G Y. Numerical simulation of multi-point forming for plate. *Jilin University*, 2004

[18] Chen J L, Li Z X, Shu W Y, et al. Experimental study on dynamic mechanical behavior of Q345 steel under different strain rates. *Journal of southeast university (Natural science edition)*.2015; 45(6):1145-1150.
[19] Wang C T, Kinzel G, Altan T. Mathematical modeling of plane-strain bending of sheet and plate.*Journal of materials processing technology*.1993;(39):279-304.
[20] Prasad Y K D V, Somasundaram S. A mathematical model for bend-allowance calculation in automated sheet-metal bending. *Journal of materials processing technology*.1993; 39:337-356.
[21] Su S J, Hu Y, Wang C F. Research on prediction model of hull plate bending springback based on SVM. *Ship science and technology*.2015; 37(5):104-108.
[22] Mei X M, Huang J Z. *Differential Geometry.* Beijing. People's education Press, 1981.
[23] Wu J Q, Yang D Y, Shen L Y. Research on the curve fitting method based on curvature data. *Journal of applied sciences*.2003; 21(3):258-262.
[24]Hashemian A, Hosseini S F. An integrated fitting and fairing approach for object reconstruction using smooth NURBS curves and surfaces. *Computers&mathematics with applications.*2018; 76(7):1555-1575.
[25] Wang C, Zhang Z L. Numerical Simulation of U-shaped Bending Springback of Two-dimensional Sheets. *Metal forming technology*.1999; 17:33-35.
[26] CATIA V5 web site. https://www.3ds.com/products-services/catia/

Corresponding author:

Shaojuan Su: Naval Architecture and Ocean Engineering College,
Dalian Maritime University, 116026, Dalian Liaoning, China;
E-mail:ssjlpz@dlmu.edu.cn
32248522@qq.com